Molecular Rotation in Self-Assembled Multidecker Porphyrin Complexes

Hiroyuki Tanaka,[†,*] Tomohiro Ikeda,[‡] Masayuki Takeuchi,[§,*] Kazuki Sada,[∥] Seiji Shinkai,[⊥,#] and Tomoji Kawai[†]

[†]The Institute of Scientific and Industrial Research, Osaka University, Ibaraki, Osaka 567-0047, Japan, [‡]Department of Chemistry and Biochemistry, Graduate School of Engineering, Kyushu University, 744 Moto-oka, Nishi-ku, Fukuoka 819-0395 Japan, [§]Organic Nanomaterials Center, National Institute for Materials Science, 1-2-1 Sengen, Tsukuba 305-0047 Japan, [∥]Department of Chemistry, Faculty of Science, Hokkaido University, North 10, West 8, Sapporo, Hokkaido, 060-0810 Japan, [⊥]Department of Nanoscience, Faculty of Engineering, Sojo University, 4-22-1 Ikeda, Kumamoto 860-0082, Japan, and [#]Institute of Systems, Information Technologies and Nanotechnology, 203-1 Moto-oka, Nishi-ku Fukuoka 819-0385 Japan

ABSTRACT

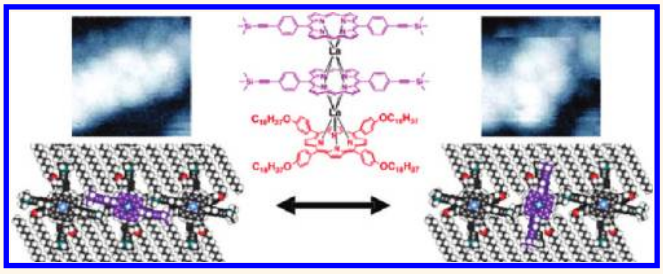

An alkyl chain-substituted multidecker porphyrin (a cerium double-decker porphyrin (CeDDP) and a lanthanum triple-decker porphyrin (LaTDP)) complexes were arranged in a monolayer array on Au(111) substrate. By using a pulse injection deposition method, both multidecker complexes were deposited on the surface intact to form a well-defined two-dimensional array. Low-temperature scanning tunneling microscopy (STM) allowed the measurement of the topographic heights of the multidecker porphyrin complexes and visualization of their internal structures clearly. The STM images suggest that the top porphyrin ligand in CeDDP rarely rotates under nondestructive imaging condition, while the top porphyrin ligand in LaTDP exhibits flip-flop rotation even under the nondestructive imaging condition at sub-pA tunneling currents. These results provide the future applications of molecular-scale mechanical machines and single molecule storage memory.

KEYWORDS: chirality · multidecker · molecular bearing · porphyrins · rotation–oscillation · scanning tunneling microscopy · Au(111) · supramolecule

Rotating and oscillating molecular bearings are important for potential use in sensors, information transfer/storage devices and molecular machines.[1] Multidecker porphyrin complexes have attracted particular attention not only due to their characteristic optical or redox properties,[2,3] but also because they represent a complete rotor/oscillator system comprising a rotation axis of metal atom(s) between porphyrin ligands, making these molecules promising candidates for single-molecule mechanical machines.[4,5] The sandwich-type multidecker porphyrin complexes and derivatives have the advantage in that addition/substitution of the long alkyl chain to a ligand which acts as a stator permits self-assembly into an ordered monolayer array on a solid surface, thereby allowing for single molecule observation using scanning tunneling microscopy (STM).[6] Although the rotation of various single-molecule rotors have been clearly observed by STM,[7−12] there have been almost no reports detailing STM visualizations of the rotation/oscillation of such multidecker complexes.[13−16] However it is true that many studies using a different technique such as the NMR reported the rotation/oscillation of such multidecker complexes.[1,17,18] This reason mainly originates from the fact that STM requires an interaction with substrate, and there are problems associated with clean sample preparation and the imaging of these large molecules. To reduce substrate effects, triple-decker complexes may be better suited for STM observation compared to double-decker complexes due to their increased height. From NMR studies it is known that use of metal ions (rotation axis) with a large ionic radius such as lanthanum generates smaller rotation barriers compared to metal ions with a small ionic radius such as cerium.[19] Therefore, two kinds of multidecker porphyrin complexes with different associated rotation barriers were chosen; a cerium double-decker porphyrin complex (tetrakis(*n*-octadecyloxyphenyl)porphyrin/tetrakis(4-aminophenyl)porphyrin/cerium ion; **DD**) and lanthanum triple-decker porphyrin complex (tetrakis(*n*-octadecyloxyphenyl) porphyrin/[bis(4-trimethylsilylethynylphenyl)porphyrin]$_2$/lanthanum ion; **TD**), shown in Figure 1 structures a and b, respectively (see Supporting

* Address correspondence to hrtanaka@sanken.osaka-u.ac.jp, TAKEUCHI.Masayuki@nims.go.jp.

Received for review July 25, 2011 and accepted November 4, 2011.

Published online November 10, 2011
10.1021/nn203773p

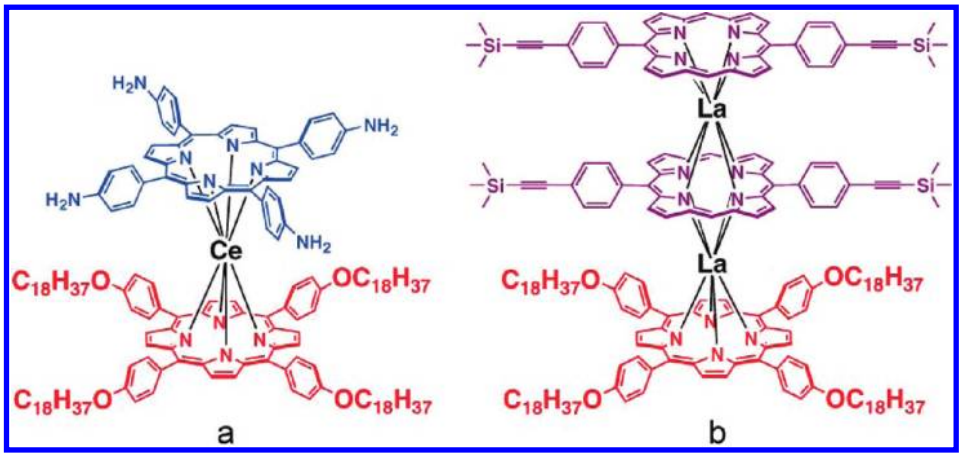

Figure 1. Molecular structure of multidecker porphyrin complexes. (a) Molecular structure of cerium(IV) double-decker porphyrin complex (tetrakis(*n*-octadecyloxyphenyl)porphyrin/tetrakis(aminophenyl)porphyrin/cerium ion; DD). (b) Molecular structure of lanthanum(III) triple-decker porphyrin complex (tetrakis(*n*-octadecyloxyphenyl)porphyrin/2-bis-(trimethylsilylethynylphenyl)porphyrin/lanthanum ion; TD).

Information for syntheses). The rotor porphyrin ligands of **DD** and **TD** possess aminophenyl substituents and trimethylsilylethynylphenyl groups at the *meso*-position, respectively, so that the stop positions (rotation angle) of the rotor differ between **DD** and **TD**. To ensure that the rotors face toward the vacuum side (face on adsorption) and comprise a well-ordered monolayer array, the stator ligand porphyrins of both samples possess a long alkyl chain (*n*-$C_{18}H_{37}$, *n*-octadecyl).

Here, we report on the distinct STM visualization of the rotation−oscillation rotor of an alkyl chain substituted multidecker porphyrin complex arranged in a monolayer array on Au(111) substrate. The combination of molecular design with alkyl chain assisted self-assembly and an originally developed sample deposition method for pyrolytic supramolecules allows STM to clearly visualize the well-defined array of single-molecular rotors. The rotor ligand has two stable stations that originate from the rotation−oscillation isomers, and is oscillated by reversibly changing the chirality in the self-assembled array.

Figure 2a shows a typical high resolution STM image of **DD** deposited on Au(111) using our own pulse injection deposition method[20−26] (see Experimental and Theoretical Methods) One can see the well-ordered array comprising four-leafed porphyrin ligands. This characteristic array is routinely reproduced in the long alkyl chain substituted porphyrin/porphyrin-derivative−substrate system, as reported in the literature.[27] The alkyl chains that interdigitate vertically between porphyrin complex rows can be seen in the contrast adjusted image of Figure 2a (see Supporting Information, Figure S1). We also found out that the periodic structure of **DD** and the free-base porphyrin with the long alkyl chain are almost identical, and the amino appended free-base porphyrin without the alkyl chain substitution does not form an array structure (see Supporting Information, Figure S2). From the above results, we determined that **DD** engages in face-on adsorption due to the alkyl chain substituted porphyrin ligand being adsorbed onto the substrate, and the amino appended porphyrin ligand without the alkyl chain substitution faces toward the vacuum. Thus, we succeeded in the formation of a two-dimensional array structure comprising a double-decker porphyrin complex on Au(111) using our original sample preparation method.

An important point is that our sample preparation method and clean STM imaging allowed for the differentiation of rotational chirality of individual **DD** molecules. Except a few recent reports on phtalocyaninato complex,[15,16,28−33] no reports to date have provided clear submolecular resolution STM images of double-decker porphyrin (derivatives) in an array. Because of the submolecular resolution images obtained here, individual **DD** molecules can be classified into one of the two rotational isomer models, minus or plus, which can be mutually changed *via* rotation−oscillation as shown in Figure 2 structures a (right) and b.

Figure 2c shows the rotational potential energy profile for **DD**, obtained using Insight II (MSI Inc.) molecular mechanics (MM) simulation, predicting that these two isomers are energetically identical and isolated by a very shallow potential barrier. The population of minus and plus (Figure 2a) is 24:24 and agrees well with this MM simulation. The big barriers at 0 and 90 degrees and a very shallow barrier at 45 degree arise from steric repulsion between the phenyl moieties and the phenyl and pyrrole moieties of the porphyrin skeleton. Note that both porphyrin ligands of **DD** possess phenyl groups at all *meso*-positions of the porphyrin skeleton. In the solution phase the thermal noise at room temperature allows for free rotation of **DD** and an equal population of minus and plus. Following deposition by pulse injection onto the Au(111) substrate, the chiral population of **DD** remains

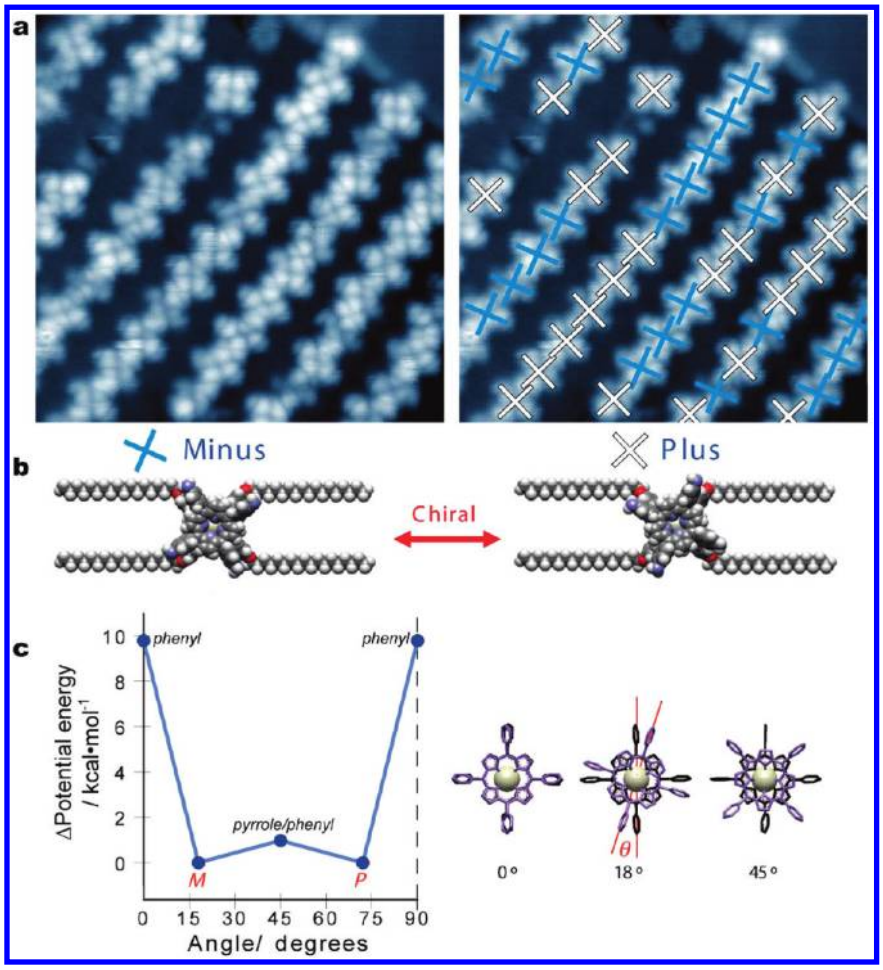

Figure 2. Array of DD on Au(111) and chirality of the top porphyrin. (a) STM image of self-assembled DD adsorbed on Au(111). Imaging conditions, $X = 20$ nm, $I = 2$ pA, $V = 1.5$ V. Two types of orientation of the top porphyrin ligand can be seen. (Right) Assignment of chirality of the top porphyrin ligand in the STM image. (b) Space-filling models of the molecule depicting minus (left) and plus (right) chirality. (c) Rotational potential energy curves for DD; energy curves obtained using Insight II (MSI Inc.) molecular mechanics simulation. (Right) The three models show definition of the angle; the eclipse position is 0°.

unchanged during the formation of two-dimensional array, and the original chiral population present in solution is maintained.

Neither the rotation nor the oscillation of the top porphyrin ligand of **DD** was observed under nondestructive STM imaging conditions (1 pA and 2 V). Gimzewski *et al*. reported that irradiation with high voltage (*ca*. 2−3 V) and high currents (2−3 nA) induced degradation of porphyrin.[34] In an effort to gradually increase the perturbation of the molecule, the STM imaging bias voltage was gradually raised (*ca*. 2.5−3.75 V) while keeping the tunneling current constant (∼pA). As a result, reorientation of the top porphyrin ligand was observed with high voltage scanning, as shown in Figure 3. Prior to high voltage scanning, no movement was observed in the STM image; scanned with V_s = 2.5 V (Figure 3a,d). When imaging with high bias voltage (V_s = 3 V), the top porphyrin ligand marked with a white dotted square changed orientation during scanning (Figure 3b,e). As with the cropped images (Figure 3d,e) and molecular models (Figure 3g), the molecule initially adopted a minus chirality which suddenly changed to plus during scanning, indicated with the pair of red arrows (Figure 3e). Note that the STM Y scanning goes from up to low in Figure 3a−c and from upper left to lower right in Figure 3d−f (see Supporting Information; Figure S3). The following STM image (Figure 3c and f) taken with a lower bias of 2 V shows that the molecule now completely adopts a plus chirality. **DD** molecules were also observed to change chirality from plus to minus (see Supporting Information; Figure S4). Considering the potential application of molecular chirality to read−write memory or rotor devices, reorientation of such molecules should preferably be reversible. Unfortunately, reversion of the reoriented **DD** molecule shown in Figure 3 and Supporting Information, Figure S5 back to its original chiral form was not observed. This may be partly due to the high bias voltage employed (3 V) which causes rotation of the top porphyrin ligand as well as damage to the **DD** molecule.[34]

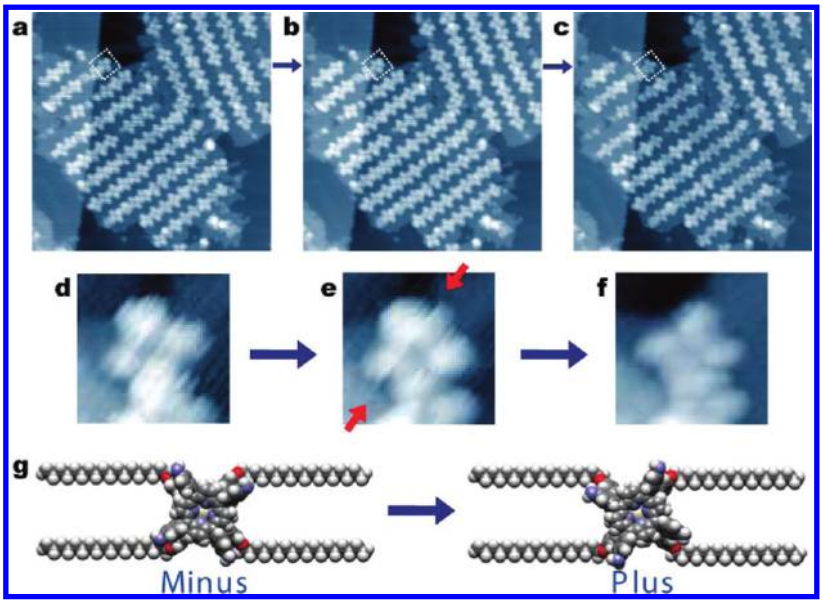

Figure 3. Reorientation of the top porphyrin ligand of DD Series of consecutive large scale (40 nm) STM images (a−c) and cropped (4 nm) images (d−f) of panels a−c; imaging conditions: (a and d) $I = 2$ pA, $V = 2.5$ V, (b and e) $I = 2$ pA, $V = 3$ V, (c and e) $I = 2$ pA, $V = 2$ V. Rotated dotted squares in panels a−c indicate cropped area. Note that the STM scanning direction is rotated in the cropped images due to the rotated selection of the area. Red arrows in panel e indicate the abrupt change in chirality (reorientation) of the top porphyrin ligand during the scan. (g) Space-filling models of the molecule show the change in chirality from minus (left) to plus (right).

We expect that the top ring of **TD** rotates more freely than **DD** since **TD** possesses aa lanthanum metal ion and porphyrin ligand, making the porphyrin ligand interactions weak. We have observed not only reorientation but also flaking off of the top ring of **TD** molecules (see Supporting Information; Figure S5). In an effort to minimize perturbation of the molecule as much as possible, the tunnel current was reduced to 0.2 pA and the voltage was −2.5 V. Figure 4 panels a and b show typical high resolution wide area and higher resolution STM images of **TD** islands, respectively. As shown in the cross section below Figure 4a, **TD** molecules have an apparent height of *ca.* 1 nm above the clean Au(111)surface, which is in good agreement with the previously reported value (*ca.* 1 nm) of a face-on adsorbed triple-decker.[35] Like **DD**, **TD** also formed a two-dimensional array structure in the islands. Since the alkyl chain of the bottom porphyrin ligands can be seen between the rows in Figure 4b, the main driving force of this self-assembled array formation is derived from the long alkyl chain substitution.[27]

The individual top layer porphyrin ligand of TD appears more like a rhombus rather than a four-leafed square as in the case of **DD**. This observed submolecular shape is consistent with the fact that the top porphyrin ligand of **TD** possesses 2-fold symmetry (see Figure 1b). An interesting point is that the orientation of the rhombus-shaped top porphyrin ligand of **TD** is almost unique in an island, that is, homochiral. Since the chirality of the porphyrin ligand of the middle and bottom layer (rotation isomer) underneath the top porphyrin ligand could not be visualized, the chirality of the entire **TD** molecule could not be completely determined. Here, we use the term clockwise (CW) and anticlockwise (ACW), *in lieu* of plus and minus, to describe the orientation of the top porphyrin ligand (see Supporting Information, Figure S5 for a definition). It is impossible to determine the chirality of even the top porphyrin when the STM tip is not of sufficient quality. However, the observed homochirality of the islands is useful in delineating the chirality of the top porphyrin ligand even when the STM tip is not ideal (see Supporting Information, Figure S5). In kink sites generated by chance flaking of the top porphyrin ligand during a previous scan, the middle porphyrin ligands could be barely seen, indicating that the orientation is perpendicular to the row. Assuming this direction is the case for intact **TD** and considering the observed orientation of the long alkyl chains (see Supporting Information, Figure S6), the molecular model of 9 **TD** molecules is successfully reproduced by the MM simulation; the top and side view of the optimized model are shown in Figure 4 panels c and d, respectively. The three component molecular layers of this model, the bottom, middle, and top, are shown in Figure 4 panels e, f, and g, respectively.

We were able to observe reversible reorientation of the top porphyrin ligand labeled **A** and **B** in Figure 4b. Figure 5a−c and 5d−f show that the top porphyrin ligands **A** and **B** in Figure 4b reoriented from ACW

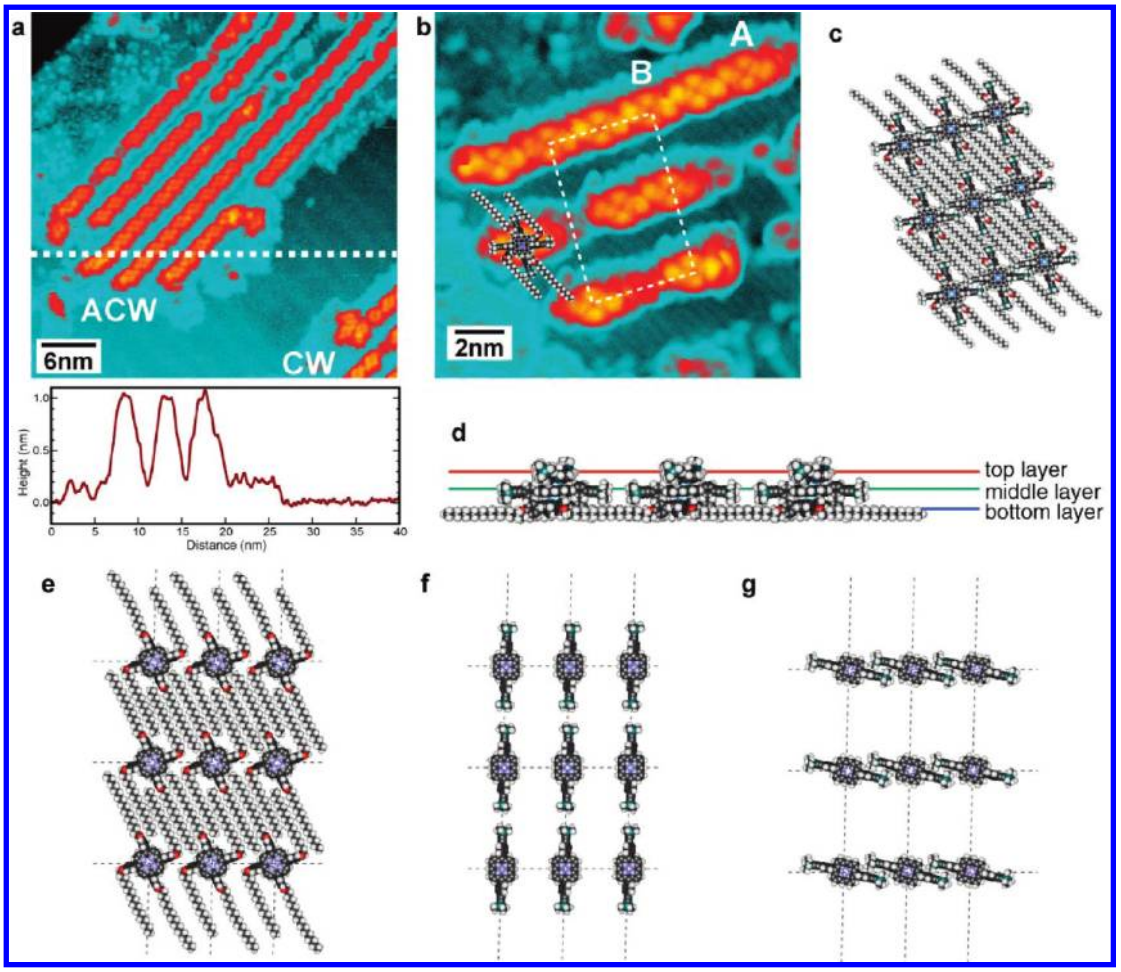

Figure 4. STM images and molecular models of TD array. (a) STM image of islands of self-assembled TD array adsorbed on Au(111); imaging conditions: *X* = 40 nm, *I* = 0.2 pA, *V*= −2.5 V. The herringbone reconstruction is seen in the open space between two islands (upper middle and lower right). A cross section of the image indicated with dotted white line shows the topographic height of TD from the bare Au(111) substrate. ACW and CW refer to anticlockwise and clockwise, respectively. A detailed definition is given in the Supporting Information (Figure S4). (b) Higher resolution STM image of island of self-assembled TD array adsorbed on Au(111); imaging conditions: *X* = 15 nm, *I* = 0.5 pA, *V*= −2 V. Closely packed alkyl chains are seen in the background of the porphyrin complex array. Space-filling model of a single TD molecule is superimposed in the middle left molecule as an example. (c−g) Space-filling models of TD molecule(s) optimized using molecular mechanics simulation: (c,d) unit cell of TD array; top view (c) and side view (d); (e−g) The top view model of each layer of the unit cell; the bottom layer (e), middle layer (f), and top layer (g).

to CW and back again from CW to ACW, respectively. Since there was no noticeable change in the molecular images of the top porphyrin ligands prior to (a and d) and following reorientation (c and f), we conclude that the observed reorientation process is reversible and nondestructive. The aforementioned nondestructive reversible rotation−oscillation can easily be understood from a movie composed of snapshots of consecutive STM images of the area covering both **A** and **B** (see Supporting Information video and Figure S7). The observed rotation angle is approximately 90 deg. This value is in good agreement with the results obtained from the MM calculation using 3 by 3 **TD** molecules. Figure 5 panels g and h depict only the center row of the optimized models, and show that the ACW position represents the energetically favorable local minimum. Reversible and nondestructive oscillation of the top porphyrin ligands (without changes in the molecular shape) suggests that there is no degradation of the molecule.

In an effort to further investigate the mechanism of the observed rotation−oscillation, we recorded consecutive STM images using the same feedback parameters and different scanning directions; *X* scan (from left to right) and *Y* scan (from bottom to top) shown respectively in Figure 5 panels i and j. The discontinuous molecular image indicated by the arrows show a temporary stop at CW, with the top rings remaining at CW for a longer period of time with the *Y* scan compared to the *X* scan. Since all of the imaging parameters were the same except for the scan direction, we conclude that the observed rotation−oscillation is induced by the STM tip scan. Although the detailed mechanism of the observed tip-induced reorientation is unclear, we have distinctly visualized the rotation−oscillation of individual multidecker porphyrin.

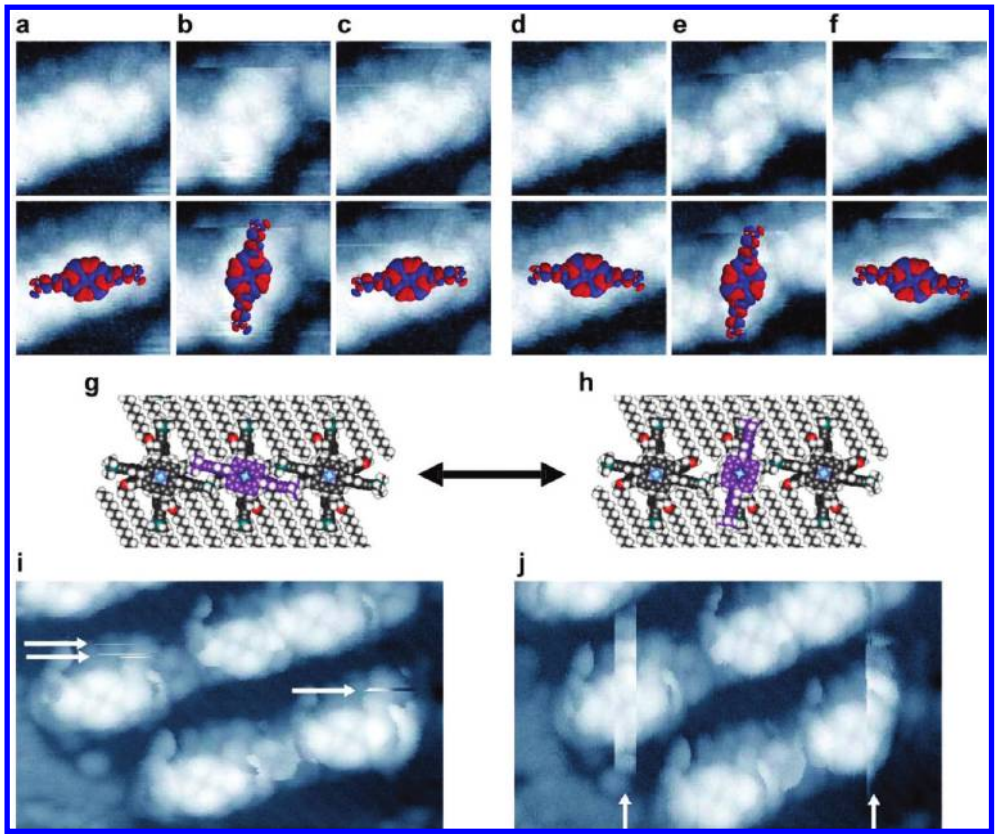

Figure 5. Oscillation of TD. The upper porphyrin ligands change orientation respectively. (a−c and d−f) Two sets of consecutive STM images (4 nm square) of the TD molecule marked A and B in Figure 4b, respectively; imaging conditions: a, I = 0.5 pA, V = −2.9 V; b and c, I = 0.5 pA, V = −2.5 V; d, I = 0.5 pA, V = −1.8 V; e, I = 0.5 pA, V = −1.7 V; f, I = 0.5 pA, V = −2 V. Structural models with molecular orbitals (HOMO and HOMO-1) of the topmost porphyrin (free base) of TD are superimposed to show the molecular orientation. This was obtained by calculating the geometry of the gas phase topmost free base porphyrin of TD with the Spartan 08 software package at the B3LYP level of theory using the 631G* basis set. Space-filling model of a single TD molecule prior to (g) and following (h) reorientation. Both models are optimized using molecular mechanics simulation. The oscillating porphyrin ligand is colored purple. (i,j) Scanning direction dependence of oscillation. To investigate the mechanism of oscillation, scan directions X (i) and Y (j) are examined in the consecutive imaging. Except for the scan directions, the two images were recorded with identical currents (I = 0.5 pA) and bias (V = −1.6 V). White arrows indicate temporary reorientation.

In summary, **DD** was sufficiently adsorbed onto the substrate to permit reorientation of the top porphyrin ligand by relatively high bias voltages that might damage the molecular system. The top porphyrin ligand of the thicker **TD** was reversibly rotation-oscillated by small perturbation from the STM imaging. We have provided unequivocal evidence of rotation−oscillation of an individual supramolecular bearing, multidecker porphyrin complex self-assembled on a solid surface using our sample deposition method. The structure of the self-assembled array and function of the supramolecules can be controlled by recently advanced molecular design methods. We expect our report to encourage further research in the area of surface mounted molecular-scale mechanical machines, as well as in areas concerning memory storage or emergent allosteric recognition systems.[36]

EXPERIMENTAL AND THEORETICAL METHODS

STM experiments were performed in an ultrahigh vacuum (below 1×10^{-10} Torr) using a low-temperature microscope (USM-1200S2N1, Unisoku Japan). The sample bias varied from −3 to 4 V with a tunneling current ranging from 0.2 pA to 2 pA. Unless otherwise indicated, images were acquired with a $Pt_{0.8}Ir_{0.2}$ tip scanning from left to right (X direction). The scan rate was maintained at ∼1 line/s. The Au(111) surface was prepared by several cycles of annealing at 750 K and sputtering with Ar+. A clean Au(111) substrate was located just under the pulse valve. The distance from the pulse valve to the substrate was 130 mm. **DD** and **TD** were respectively dissolved in chloroform at concentrations in the range of 0.1−1 mM. The solution was injected toward the substrate at room temperature when the valve was opened for ∼1 ms.[20−26] The amount per dose is approximately sub-microliter. In all experiments presented, sample was transferred to a liquid nitrogen-cooled (*ca.* 80 K) STM head. Molecular conformations were optimized using the Insight II (Molecular Simulations Inc.) semiempirical program.

Acknowledgment. We thank Prof. Toru Ide of the Network Center for Molecular and System Life Sciences, Graduate School of Frontier Biosciences, Osaka University, for mediating the collaboration. We also thank Prof. K. W. Hipps of Washington State University and Prof. Tomohide Takami of Konkuk University for their comments on the manuscript. This work was supported by the Ministry of Education, Culture, Sports, Science and Technology of Japan (MEXT) *via* Grant-in-Aids for "Molecular and System Life Science" and for Scientific Research on Innovative Areas "Emergence in Chemistry" (20111007 to H.T.) and on "Coordination Programming" (21108010 to M.T.).

Supporting Information Available: Syntheses, supporting figures (Figure S1–S7), and video. This material is available free of charge *via* the Internet at http://pubs.acs.org.

REFERENCES AND NOTES

1. Tashiro, K.; Fujiwara, T.; Konishi, K.; Aida, T. Rotational Oscillation of Two Interlocked Porphyrins in Cerium Bis-(5,15-diarylporphyrinate) Double-Deckers. *Chem. Commun.* **1998**, 1121–1122.
2. Bilsel, O.; Rodriguez, J.; Holten, D. Picosecond Relaxation of Strongly Coupled Porphyrin Dimers. *J. Phys. Chem.* **1990**, *94*, 3508–3512.
3. Buchler, J. W.; Scharbert, B. Metal Complexes with Tetrapyrrole Ligands. 50. Redox Potentials of Sandwichlike Metal Bis(Octaethylporphyrinates) and Their Correlation with Ring–Ring Distances. *J. Am. Chem. Soc.* **1988**, *110*, 4272–4276.
4. Kottas, G. S.; Clarke, L. I.; Horinek, D.; Michl, J. Artificial Molecular Rotors. *Chem. Rev.* **2005**, *105*, 1281–1376.
5. Tashiro, K.; Konishi, K.; Aida, T. Enantiomeric Resolution of Chiral Metallobis(Porphyrin)s: Studies on Rotatability of Electronically Coupled Porphyrin Ligands. *Angew. Chem., Int. Ed.* **1997**, *36*, 856–858.
6. Binnemans, K.; Sleven, J.; Feyter, S. D.; Schryver, F. C. D.; Donnio, B.; Guillon, D. Structure and Mesomorphic Behavior of Alkoxy-Substituted Bis(Phthalocyaninato)-Lanthanide(III) Complexes. *Chem. Mater.* **2003**, *15*, 3930–3938.
7. Browne, W. R.; Feringa, B. L. Making Molecular Machines Work. *Nat. Nanotechnol.* **2006**, *1*, 25–35.
8. Gimzewski, J. K.; Joachim, C.; Schlittler, R. R.; Langlais, V.; Tang, H.; Johannsen., I. Rotation of a Single Molecule within a Supramolecular Bearing. *Science* **1998**, *281*, 531–533.
9. Stipe, B. C.; Rezaei, M. A.; Ho, W. Inducing and Viewing the Rotational Motion of a Single Molecule. *Science* **1998**, *279*, 1907–1909.
10. Stipe, B. C.; Rezaei, M. A.; Ho, W. Coupling of Vibrational Excitation to the Rotational Motion of a Single Adsorbed Molecule. *Phys. Rev. Lett.* **1998**, *81*, 1263–1266.
11. Chiravalloti, F.; Gross, L.; Rieder, K.-H.; Stojkovic, S.-M.; Gourdon, A.; Joachim, C.; Moresco, F. A Rack-and-Pinion Device at the Molecular Scale. *Nat. Mater.* **2007**, *6*, 30–33.
12. Manzano, C.; Soe, W.-H.; Wong, H. S.; Ample, F.; Gourdon, A.; Chandrasekhar, N.; Joachim, C. Step-by-Step Rotation of a Molecule-Gear Mounted on an Atomic-Scale Axis. *Nat. Mater.* **2009**, *8*, 576–579.
13. Lei, S.-B.; Deng, K.; Yang, Y.-L.; Zeng, Q.-D.; Wang, C.; Jiang, J.-Z. Electric Driven Molecular Switching of Asymmetric Tris(Phthalocyaninato) Lutetium Triple-Decker Complex at the Liquid/Solid Interface. *Nano Lett.* **2008**, *8*, 1836–1843.
14. Otsuki, J.; Komatsu, Y.; Kobayashi, D.; Asakawa, M.; Miyake, K. Rotational Libration of a Double-Decker Porphyrin Visualized. *J. Am. Chem. Soc.* **2010**, *132*, 6870–6871.
15. Komeda, T.; Isshiki, H.; Liu, J.; Zhang, Y.-F.; Lorente, N.; Katoh, K.; Breedlove, B. K.; Yamashita, M. Observation and Electric Current Control of a Local Spin in a Single-Molecule Magnet. *Nat. Comms.* **2011**, *2*, 217–223.
16. Écija, D; Auwärter, W; Vijayaraghavan, S; Seufert, K; Bischoff, F; Tashiro, K; Barth, J. V. Assembly and Manipulation of Rotatable Cerium Porphyrinato Sandwich Complexes on a Surface. *Angew. Chem., Int. Ed.* **2011**, *50*, 3872–3877.
17. Tashiro, K.; Konishi, K.; Aida, T. Enantiomeric Resolution of Chiral Metallobis(Porphyrin)s: Studies on Rotatability of Electronically Coupled Porphyrin Ligands. *Angew. Chem., Int. Ed.* **1997**, *36*, 856–858.
18. Takeuchi, M.; Imada, T.; Ikeda, M.; Shinkai, S. Ring Rotation Controversy in Cerium(IV) Bis(tetraarylporphyrinate) Double Deckers: HPLC Evidence for the Question to Rotate or Not Roatate. *Tetrahedron Lett.* **1998**, *39*, 7897–7900.
19. Ikeda, M.; Takeuchi, M; Shinkai, S.; Tani, F.; Naruta, Y. Synthesis of New Diaryl-Substituted Triple-Decker and Tetraaryl-Substituted Double-Decker Lanthanum(III) Porphyrins and Their Porphyrin Ring Rotational Speed as Compared with that of Double-Decker Cerium(IV) Porphyrins Porphyrin Ring Rotational Speed. *Bull. Chem. Soc. Jpn.* **2001**, *74*, 739–746.
20. Tanaka, H.; Kawai, T. Scanning Tunneling Microscopy Imaging and Manipulation of DNA Oligomer Adsorbed on Cu(111) Surfaces by a Pulse Injection Method. *J. Vac. Sci. Technol.* **1997**, *B 15*, 602–604.
21. Tanaka, H.; Hamai, C.; Kanno, T.; Kawai, T. High-Resolution Scanning Tunneling Microscopy Imaging of DNA Molecules on Cu(111) Surfaces. *Surf. Sci.* **1999**, *432*, L611–L616.
22. Sugiura, K.-i; Tanaka, H.; Mastumoto, T.; Kawai, T.; Sakata, Y. A Mandala-Patterned *Bandanna*-Shaped Porphyrin Oligomer, $C_{1244}H_{1350}N_{84}Ni_{20}O_{88}$, Having a Unique Size and Geometry. *Chem. Lett.* **1999**, 1193–1194.
23. Tanaka, H.; Kawai, T. Visualization of Detailed Structures within DNA. *Surf. Sci.* **2003**, *539*, L531–L536.
24. Kato, A.; Sugiura, K.-i; Miyasaka, H.; Tanaka, H.; Kawai, T. A Square Cyclic Porphyrin Dodecamer: Synthesis and Single-Molecule Characterization. *Chem. Lett.* **2004**, *33*, 578–579.
25. Tanaka, H.; Kawai, T. Partial Sequencing of a Single DNA Molecule with a Scanning Tunnelling Microscope. *Nat. Nanotechnol.* **2009**, *4*, 518–522.
26. Yamashita, K.-i; Akita, Y.; Asano, M. S.; Tanaka, H.; Kawai, T.; Sugiura, K.-i. A Proposal for a New Porphine Substitution Motif Aimed at Advanced Materials: Introduction of 4-alkoxy-3,5-Diisopropylphenyl Groups on Porphine. *J. Porphyrins Phthalocyanines* **2010**, *14*, 1040–1051.
27. Ikeda, T.; Asakawa, M.; Goto, M.; Miyake, K.; Ishida, T.; Shimizu., T. STM Observation of Alkyl-Chain-Assisted Self-Assembled Monolayers of Pyridine-Coordinated Porphyrin Rhodium Chlorides. *Langmuir.* **2004**, *20*, 5454–5459.
28. Zhang, Y. F.; Isshiki, H.; Katoh, K.; Yoshida, Y.; Yamashita, M.; Miyasaka, H.; Breedlove, B. K.; Kajiwara, T.; Takaishi, S.; Komeda, T. Low-Temperature Scanning Tunneling Microscopy Investigation of Bis(Phthalocyaninato)Yttrium Growth on Au(111): From Individual Molecules to Two-Dimensional Domains. *J. Phys. Chem. C.* **2009**, *113*, 9826–9830.
29. Katoh, K.; Yoshida, Y.; Yamashita, M.; Miyasaka, H.; Breedlove, B. K.; Kajiwara, T.; Takaishi, S.; Ishikawa, N.; Isshiki, H.; Zhang, Y. F.; *et al.* Direct Observation of Lanthanide(III)-Phthalocyanine Molecules on Au(111) by Using Scanning Tunneling Microscopy and Scanning Tunneling Spectroscopy and Thin-Film Field-Effect Transistor Properties of Tb(III)- and Dy(III)-Phthalocyanine Molecules. *J. Am. Chem. Soc.* **2009**, *131*, 9967–9976.
30. Isshiki, H.; Liu, J.; Katoh, K.; Yamashita, M.; Miyasaka, H.; Breedlove, B. K.; Takaishi, S.; Komeda, T. Scanning Tunneling Microscopy Investigation of Tris(Phthalocyaninato)-Yttrium Triple-Decker Molecules Deposited on Au(111). *J. Phys. Chem. C.* **2010**, *114*, 12202–12206.
31. Katoh, K.; Komeda, T.; Yamashita, M. Surface Morphologies, Electronic Structures, and Kondo Effect of Lanthanide(III)-Phthalocyanine Molecules on Au(111) by using STM, STS and FET Properties for Next Generation Devices. *Dalton Trans.* **2010**, *39*, 4708–4723.

32. Katoh, K.; Isshiki, H.; Komeda, T.; Yamashita, M. Multiple-Decker PhthalocyaninatoTb(III) Single-Molecule Magnets and Y(III) Complexes for Next Generation Devices. *Coord. Chem. Rev.* **2011**, *255*, 2124–2148.
33. Toader, M.; Knupfer, M.; R. T. Zahn, D.; Hietschold, M. Initial Growth of Lutetium(III) Bis-phthalocyanine on Ag(111) Surface. *J. Am. Chem. Soc.* **2011**, *133*, 5538–5544.
34. Gimzewski, J. K.; Jung, T. A.; Cuberes, M. T.; Schlittler, R. R. Scanning Tunneling Microscopy of Individual Molecules: Beyond Imaging. *Surf. Sci.* **1997**, *386*, 101–114.
35. Tanaka, H.; Ikeda, T.; Yamashita, K.; Takeuchi, M.; Shinkai, S.; Kawai, T. Network of Tris(Porphyrinato)Cerium(III) Arranged on the Herringbone Structure of an Au(111) Surface. *Langmuir* **2010**, *26*, 210–214.
36. Takeuchi, M.; Ikeda, M.; Sugasaki, A.; Shinkai, S. Molecular Design of Artificial Molecular and Ion Recognition Systems with Allosteric Guest Responses. *Acc. Chem. Res.* **2001**, *34*, 865–873.